Multiplet of Skyrmion States on a Curvilinear Defect: Reconfigurable Skyrmion Lattices

Volodymyr P. Kravchuk,[1,2,*] Denis D. Sheka,[3,†] Attila Kákay,[4,‡] Oleksii M. Volkov,[4,§] Ulrich K. Rößler,[2,‖]
Jeroen van den Brink,[2,5,¶] Denys Makarov,[4,**] and Yuri Gaididei[1,††]

[1]*Bogolyubov Institute for Theoretical Physics of National Academy of Sciences of Ukraine, 03680 Kyiv, Ukraine*
[2]*Leibniz-Institut für Festkörper- und Werkstoffforschung, IFW Dresden, D-01171 Dresden, Germany*
[3]*Taras Shevchenko National University of Kyiv, 01601 Kyiv, Ukraine*
[4]*Helmholtz-Zentrum Dresden—Rossendorf e.V., Institute of Ion Beam Physics and Materials Research, 01328 Dresden, Germany*
[5]*Institute for Theoretical Physics, TU Dresden, 01069 Dresden, Germany*

Typically, the chiral magnetic Skyrmion is a single-state excitation. Here we propose a system, where multiplet of Skyrmion states appears and one of these states can be the ground one. We show that the presence of a localized curvilinear defect drastically changes the magnetic properties of a thin perpendicularly magnetized ferromagnetic film. For a large enough defect amplitude a discrete set of equilibrium magnetization states appears forming a ladder of energy levels. Each equilibrium state has either a zero or a unit topological charge; i.e., topologically trivial and Skyrmion multiplets generally appear. Transitions between the levels with the same topological charge are allowed and can be utilized to encode and switch a bit of information. There is a wide range of geometrical and material parameters, where the Skyrmion level has the lowest energy. Thus, periodically arranged curvilinear defects can result in a Skyrmion lattice as the ground state.

Introduction.—Skyrmions are common in nature. Having arisen in particle physics [1], the notion of these topological excitations is now used for liquid crystals [2], Bose-Einstein condensates [3,4], and magnetically ordered systems [5–8]. During the few last years, magnetic Skyrmions have been widely considered as data carriers in spintronic data storage and logic devices [7–16]. In contrast to individual Skyrmions, their periodic 2D arrays, i.e., Skyrmion lattices [17–21], are relevant for electronics, relying on the topological properties of materials. In this regard, dense lattices of small-sized Skyrmions facilitate the signal readout in prospective spintronic devices by enhancing the topological Hall effect [22–25]. Typically, Skyrmion lattices are in-field low temperature pocket phases [17–20] that hinder their application potential. For this reason, much effort was made to create artificial Skyrmions and their lattices [26–30]. The puzzling, and yet unanswered, question is if there are systems with several Skyrmion levels allowing transitions between them. Furthermore, there is an intensive search for the systems where Skyrmions can form a ground state [10,31,32].

Here we show that a Skyrmion can form a ground state when its radius is comparable with the size of curvilinear defect of the magnetic film. Therefore, a periodically arranged lattice of the defects can generate a Skyrmion lattice as a ground state. This Skyrmion lattice exists in the zero magnetic field and for a temperature regime, which allows individual Skyrmions, e.g., for room temperatures [33,34]. A promising feature of the proposed curvature

induced Skyrmion lattice is its reconfigurability, which originates from the fundamentally new property of the Skyrmion pinned on the curvilinear defect. We demonstrate that in this case, a Skyrmion can have two or more equilibrium states with a very different Skyrmion radius; i.e., one deals with a multiplet of Skyrmion states. Remarkably, one of these Skyrmion states can have the lowest energy in the system. The effect of multiplicity of Skyrmion states and allowed reversible transitions between them is the main result of this paper.

The full scale micromagnetic simulations using TetraMag [35] perfectly confirms our theoretical predictions: the shape and energies of the Skyrmions, switching between different Skyrmion states by means of the external field pulse. Reconfigurability of the Skyrmion lattices opens a new exciting perspective for the manipulation and control of spintronic devices relying on the topological Hall effect [22–25].

Model.—Topologically nontrivial radial configurations can be stabilized by various interactions. Circular or bubble domains are stabilized by the nonlocal magnetostatic interactions [36–39]. Frustrated next-neighbor exchange interactions [40–42] can lead to Skyrmion formation, which can be modified with high frequency light [43]. Here, we focus on chiral Skyrmions [6,39], whose structure, similar to the well-studied planar case [6,44–48], is mainly determined by the competition of three local interactions: exchange, easy-normal anisotropy, and Dzyaloshinskii-Moriya interaction (DMI). Thus, the energy functional of our model reads

$$E = L \int [A\mathcal{E}_{\text{ex}} + K(1 - m_n^2) + D\mathcal{E}_D]d\mathcal{S}, \qquad (1)$$

where L is the film thickness, and the integration is performed over the film area. The first term of the integrand is the exchange energy density with $\mathcal{E}_{\text{ex}} = \sum_{i=x,y,z}(\partial_i \boldsymbol{m})^2$, and A being the exchange constant. Here $\boldsymbol{m} = \boldsymbol{M}/M_s$ is the unit magnetization vector with M_s being the saturation magnetization. The second term is the easy-normal anisotropy, where $K > 0$ and $m_n = \boldsymbol{m} \cdot \boldsymbol{n}$ is the normal magnetization component with $\boldsymbol{n}$ being the unit normal to the surface. The exchange-anisotropy competition results in the magnetic length $\ell = \sqrt{A/K}$, which determines a length scale of the system. The last term in (1) represents DMI with $\mathcal{E}_D = m_n \boldsymbol{\nabla} \cdot \boldsymbol{m} - \boldsymbol{m} \cdot \boldsymbol{\nabla} m_n$. Such a kind of DMI originates from the inversion symmetry breaking on the film interface; it is typical for ultrathin films [47,49,50] or bilayers [51], and it results in Néel (hedgehog) Skyrmions [10,52]. For a surface of rotation with a radially symmetrical magnetization distribution the same type of DMI effectively appears in the exchange term due to curvature effects [53–55]; thus, a direct competition takes place. This results in a Skyrmion solution of Néel type [56].

In our model, we disregard nonlocal magnetostatic effects. Still, in stark contrast to the planar case, this is not required for the realization of a Skyrmion lowest energy state [57]. Magnetization homogeneity along the normal direction is assumed, which is valid for $L \lesssim \ell$. The used continuous approach is physically sound for the cases when the minimal curvature radius, as well as the radius of the Skyrmion, is substantially larger than the interatomic distance.

A curvilinear defect of the film formed by a complete revolution of the curve $\boldsymbol{\gamma} = r\boldsymbol{e}_x + z(r)\boldsymbol{e}_z$ around the z axis is considered, namely a bump, see Fig. 1(d). The parameter $r \geq 0$ denotes the distance to the axis of rotation. Curvilinear properties of the surface at each point are completely determined by two principal curvatures k_1 and k_2, see the explicit forms in Sec. S.I in [62].

The constrain $|\boldsymbol{m}| = 1$ is utilized by introducing the spherical angular parametrization $\boldsymbol{m} = \sin\theta \cos\phi\boldsymbol{e}_s + \sin\theta \sin\phi\boldsymbol{e}_\chi + \cos\theta\boldsymbol{n}$ in the local orthonormal basis $\{\boldsymbol{e}_s, \boldsymbol{e}_\chi, \boldsymbol{n}\}$, where $\boldsymbol{e}_s$ is unit vector tangential to the curve $\boldsymbol{\gamma}$, and $\boldsymbol{e}_\chi = \boldsymbol{n} \times \boldsymbol{e}_s$ is the unit vector in azimuthal direction, see Fig. 1. Expressions for $\mathcal{E}_{\text{ex}}$ and $\mathcal{E}_D$ for a general case of a local curvilinear basis were previously obtained in Ref. [53] and Ref. [55], respectively. Without edge effects (e.g., for a closed surface or for an infinitely large film) the DMI energy density can be reduced to

$$\mathcal{E}_D = 2(\boldsymbol{\nabla}\theta \cdot \boldsymbol{\varepsilon})\sin^2\theta - \mathcal{H}\cos^2\theta, \qquad (2)$$
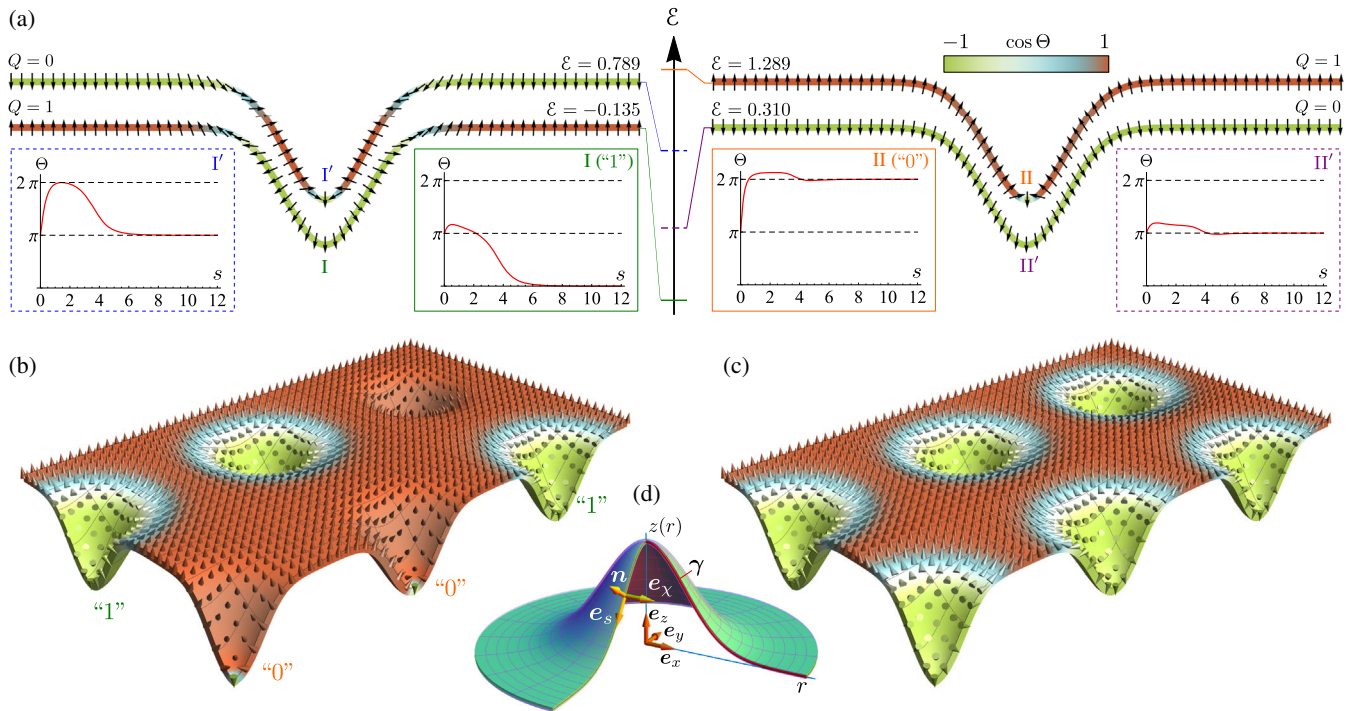

FIG. 1. *Individual Skyrmion profiles and Skyrmion lattices.* (a): Equilibrium magnetization states of a single Gaussian concave bump ($\mathcal{A} = -3$, $r_0 = 1$ and $d = 1$) are shown in a vertical cross section view. Arrows indicate the magnetization distribution and the normal component $m_n = \cos\Theta$ is color coded. The corresponding solutions $\Theta(s)$ of Eq. (3) are shown in the insets I, II, I', and II'. Vertical axis $\mathcal{E} = E/E_{\text{BP}}$ shows the distribution of the corresponding energy levels obtained from (S8) with $E_{\text{BP}} = 8\pi AL$ being energy of the Belavin-Polyakov soliton [66]. (b) Two Skyrmion states with big (I) and small (II) radii are shown on the same bumps arranged in a square lattice. These Skyrmion solutions can be considered as logical states "1" and "0" of an information bit. (c) Skyrmion lattice as a ground state. (d) Sketch of the geometry with the Cartesian $\{\boldsymbol{e}_x, \boldsymbol{e}_y, \boldsymbol{e}_z\}$ and curvilinear $\{\boldsymbol{e}_s, \boldsymbol{e}_\chi, \boldsymbol{n}\}$ frames of reference used throughout the manuscript.

where $\varepsilon = \cos\phi e_s + \sin\phi e_\chi$ is a normalized projection of the vector m on the tangential plane, and $\mathcal{H} = k_1 + k_2$ is the mean curvature. Expression (2) clearly shows the appearance of an effective DMI-driven uniaxial anisotropy proportional to the mean curvature. It has the same curvilinear origin as the recently obtained exchange-driven anisotropy and DMI [53,54]. Depending on the sign of the product $D\mathcal{H}$, this anisotropy can be of easy-normal ($D\mathcal{H} > 0$) or easy-surface ($D\mathcal{H} < 0$) type [67].

We show (see Sec. S.II) that the total energy (1) is minimized by a stationary solution $m = \sin\Theta e_s + \cos\Theta n$, where function $\Theta(s) \in \mathbb{R}$ is determined by equation

$$\nabla_s^2\Theta - \sin\Theta\cos\Theta\Xi + r'r^{-1}(d - 2k_2)\sin^2\Theta = \mathcal{H}'. \quad (3)$$

All distances are considered dimensionless and are measured in units of the magnetic length ℓ. The prime denotes the derivative with respect to the natural parameter s—the arc length along γ. The radial part of the Laplace operator reads $\nabla_s^2 f = r^{-1}(rf')'$. The function $r(s)$ unambiguously determines the surface and its curvilinear properties, see Sec. S.I. The dimensionless DMI constant $d = D/\sqrt{AK}$ is the only material parameter, which controls the system, and $\Xi = 1 + r^{-2}r'^2 - k_2^2 + d\mathcal{H}$.

It is important to note that any solution of Eq. (3) and its energy (S8) are invariant with respect to the transformation $\Theta \to \Theta + \pi$; i.e., any solution is doubly degenerate with respect to the replacement $m \to -m$ [68]. Consequently, one can fix the boundary condition $\Theta(0) = \pi$ at the bump center without the loss of generality and consider different boundary conditions at the infinity: $\Theta(\infty) = n\pi$ with $n \in \mathbb{Z}$ [69].

Following Ref. [55], one can show that the topological charge (mapping degree to S^2) of such a radially symmetrical solution on a localized bump reads (see Sec. S.III) $Q = \frac{1}{2}[\cos\Theta(\infty) - \cos\Theta(0)]$. Therefore, only $Q = 0$ (for odd n) or $Q = 1$ (for even n) values are possible. A state with $Q = -1$ appears under the transformation $m \to -m$ applied to the state with $Q = 1$.

Due to the presence of the right-hand side (rhs) driving term in Eq. (3) the trivial solutions $\Theta \equiv 0, \pi$ (i.e., $m = \pm n$) are generally not possible. It means that even for large anisotropy the magnetization vector deviates from the normal direction, except surfaces with $\mathcal{H} = \text{const}$, e.g., planar films, spherical, and minimal surfaces. Such a prediction was previously made in Ref. [53]. In 1D curvilinear wires, the analogous rhs curvature gradient results in the domain wall drift along the curvature gradient [70]. Thus, Eq. (3) reveals a leading role of the mean curvature gradient in the curvature induced Skyrmion motion.

In the planar film limit $k_1 = k_2 \equiv 0$, $\mathcal{H} \equiv 0$ and $r(s) = s$; thus, Eq. (3) is transformed into the well-known 6,45,48,52]] chiral Skyrmion equation. Such planar systems are controlled by the d parameter only. There is a critical value $d_0 = 4/\pi$, which separates two ground states, namely the uniform state $m = n$ for the case $|d| < d_0$, and helical periodical state for $|d| > d_0$ [6,45,48,52]. For the

case $|d| < d_0$, the planar form of Eq. (3) has a stable topological ($Q = 1$) solution—a Skyrmion that has the following features: (i) for a given value of d the Skyrmion solution is unique; (ii) the Skyrmion energy is always higher than energy of the uniform perpendicular state; i.e., the planar Skyrmion is an excitation of the ground state. As shown below, these well-known properties are violated in the general case of the curvilinear defect.

Gaussian bump.—As an example, we consider a class of localized curvilinear defects in form $z(r) = \mathcal{A}e^{-r^2/(2r_0^2)}$. The amplitudes $\mathcal{A} > 0$ ($\mathcal{A} < 0$) correspond to bumps that are convex (concave), and r_0 determines the bump width. In Fig. 1(a), we demonstrate stable equilibrium solutions of Eq. (3) for certain values of parameters. There is a number of principal differences as compared to the planar case: (i) Topologically nontrivial ($Q = 1$) as well as trivial ($Q = 0$) solutions are generally not unique: for given values of geometrical and material parameters a set of equilibrium magnetization states can appear with a ladder of energy levels. This makes the curvilinear defect conceptually similar to a quantum well with a finite number of discrete energy levels. However, in contrast to the quantum systems, only transitions between levels with the same Q are allowed. Such transitions are expected to be accompanied by emission or absorption of magnons. (ii) The lowest energy level can be a topological nontrivial ($Q = 1$) state stabilized by local interactions only. Therefore, curvilinear defects arranged in a periodical lattice generate a zero-field Skyrmion lattice as a ground state of the system, see Fig. 1(c).

Let us consider Skyrmions of small and big radii, which are shown in Fig. 1 as states I ("1") and II ("0"), respectively. Their radii [71] are close to extrema points of the Gauss curvature $\mathcal{K} = k_1k_2$, which plays an important role in a coupling between topological defects and curvature [72,73]. However, the radius of Skyrmion II is of one order of magnitude smaller than the radius of the Skyrmion stabilized by the intrinsic DMI in a planar film for the same value of d. Thus, the small radius Skyrmion is stabilized mostly by the curvature [55,74–76], while the big radius Skyrmion is a result of the cooperative action of the intrinsic DMI and curvature. Structures similar to the big radius Skyrmions were previously observed experimentally in Co/Pd and Co/Pt multilayer films containing an array of curvilinear defects in form of spherical concavities [77,78] as well as convexes [79,80]. The topologically trivial state I′ can be treated as a joint state of small and big radii Skyrmions, which compensate topological charges of each other. And the state II′ is an intermediate one between uniform $m = -e_z$ and normal $m = -n$ states, what reflects the competition between exchange and anisotropy interactions. Note that structures of the states I and I′, as well as states II and II′, are very close but presence or absence of the small-radius Skyrmion at the bump center. In Fig. 1(a) we show only stable solutions with $\Delta\Theta = |\Theta(\infty) - \Theta(0)| \leq \pi$. Solutions with the larger phase incursion, so called skyrmioniums [48,81] or target Skyrmions [31,46,52,82,83], are in principle also possible.
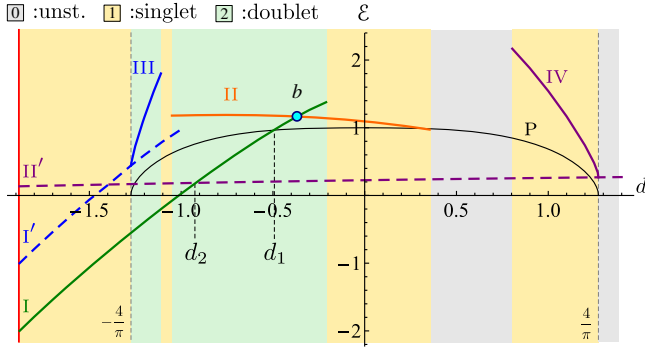
FIG. 2. *Energies of different solutions.* Solid lines I–IV and dashed lines I′, II′ show energies (S8) of topological nontrivial (Skyrmion) and trivial states, respectively, for the bump with $\mathcal{A} = 2$ and $r_0 = 1$. Energy of the planar Skyrmion is shown by the thin line P. States I, II, I′, II′ are similar to the same name states in Fig. 1. States III and IV correspond to Skyrmions whose radius much exceeds the lateral bump size, see Figs. S5 and S8. The background filling corresponds to the number of stable Skyrmion states, see also Fig. 3. For the case $d < d_2$, the Skyrmion state I has the lowest energy in the system; this corresponds to the dashed area in the Fig. 3.

FIG. 3. *Diagram of Skyrmion states for Gaussian bump with* $r_0 = 1$. In the white area, the Skyrmion solutions do not exist. The number of any other area (see legend) coincides with the number of stable Skyrmion solutions. At least one Skyrmion solution exists within the gray area "0"; however, the bump center is a position of unstable equilibrium for it. Within the other areas the corresponding number of Skyrmion are pinned at the bump center. The horizontal dashing shows areas where the lowest energy level is Skyrmion one. The star marker shows the parameters of Fig. 1. The solutions spectra for points *a–f* are presented in Sec. S.VI. The dotted horizontal line $\mathcal{A} = 2$ corresponds to Fig. 2.

The appearance of Skyrmions of type I (big radius) and type II (small radius) is a common feature of the considered curvilinear defects, and takes place for concave as well as for convex geometries. In order to illustrate the last statement, we show the energies $\mathcal{E}(d)$ for all equilibrium states, which appear for a convex bump, see Fig. 2. For the given geometrical parameters we found numerically all solutions of Eq. (3) with $\Delta\Theta \leq \pi$ for each value d. Then a stability analysis (see Sec. S.IV) was applied for each of the solutions. Finally, four stable topological (Skyrmion) solutions (lines I–IV) and two stable nontopological solutions (lines I′ and II′) are found. The magnetization distributions corresponding to all these solutions, are shown in Sec. S.VI. Lines I and II represent the above considered big ("1") and small ("0") radius Skyrmions. Remarkably, these states can have equal energies—point *b* in Fig. 2. This makes the proposed application for the storing of a bit of information more practically relevant: switching between states "0" and "1" can be easily controlled by the application of a pulse of a magnetic field directed along or against the vertical axis, see Sec. S.V and the supplemental movies. It is important that the energy, which is absorbed by the system during the process of switching from the big- to small-radius Skyrmion, is one order of magnitude lower as compared to the energy of an infinitesimally small Skyrmion: $\Delta\mathcal{E} \ll 1$, see Sec. S.V. This prevents collapse of the small Skyrmion during the switching.

As well as for the concave geometry (Fig. 1), the big radius Skyrmion on a convex bump can have the lowest energy in the system (the range $d < d_2$). It is important to note that there is a range of parameters $-4/\pi < d < d_1$
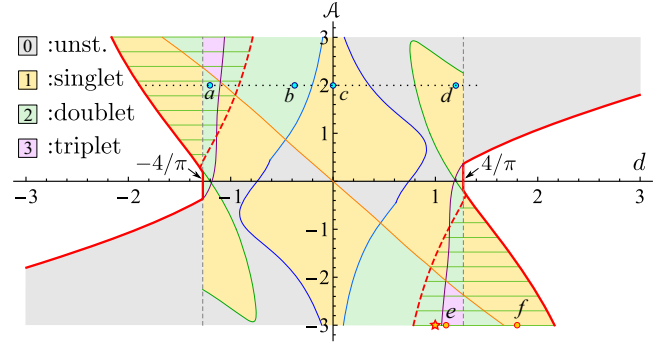
where a Skyrmion on a bump has lower energy than a planar Skyrmion for the same d. This implies that flexible enough planar films can spontaneously undergo a Skyrmion induced deformation. Such a soliton-induced magnetic film deformation was earlier predicted for cylindrical geometries [84–88].

In order to systematize possible Skyrmion solutions that can appear on Gaussian bumps, we build a diagram of Skyrmion states, see Fig. 3. We apply the same method as for the case of Fig. 2, but restricting ourselves with Skyrmion solutions. The following general features can be established: (i) The range of Skyrmions existence widens with increasing of the bump amplitude. (ii) For a wide range of parameters (gray area "0") the Skyrmion centered on the bump experiences a displacement instability because the bump center is a position of unstable equilibrium. (iii) In the vicinity of the critical value $d = \pm 4/\pi$, there is a wide area of parameters (the dashed area), where the Skyrmion state has the lowest energy in the class of radially symmetrical solutions.

Conclusions.—We have generalized the Skyrmion equation for the case of an arbitrary surface of rotation. Considering specifically a Gaussian bump we have shown that its Skyrmion solution is generally not unique—a discrete ladder of equilibrium Skyrmion states appears. We propose to use a suitably shaped curvilinear defect with a doubly degenerate Skyrmion state as carrier of a bit of information. We also predict the effect of the spontaneous deformation of an elastic magnetic film under Skyrmion influence. Finally, we found a wide range of parameters, where a Skyrmion pinned on the bump has lower energy

then other possible states. This feature can be used to generate a zero-field Skyrmion lattice as ground state.

[*]Corresponding author.
 vkravchuk@bitp.kiev.ua
[†]sheka@knu.ua
[‡]a.kakay@hzdr.de
[§]o.volkov@hzdr.de
[‖]u.roessler@ifw-dresden.de
[¶]j.van.den.brink@ifw-dresden.de
[**]d.makarov@hzdr.de
[††]ybg@bitp.kiev.ua

[1] I. Zahed and G. E. Brown, The Skyrme model, Phys. Rep. 142, 1 (1986).

[2] J.-i. Fukuda and S. Žumer, Quasi-two-dimensional Skyrmion lattices in a chiral nematic liquid crystal, Nat. Commun. 2, 246 (2011).

[3] U. Al Khawaja and H. Stoof, Skyrmions in a ferromagnetic Bose–Einstein condensate, Nature (London) 411, 918 (2001).

[4] J.-y. Choi, W. J. Kwon, M. Lee, H. Jeong, K. An, and Y.-il Shin, Imprinting Skyrmion spin textures in spinor Bose–Einstein condensates, New J. Phys. 17, 069501 (2015).

[5] N. Nagaosa and Y. Tokura, Topological properties and dynamics of magnetic Skyrmions, Nat. Nanotechnol. 8, 899 (2013).

[6] A. O. Leonov, T. L. Monchesky, N. Romming, A. Kubetzka, A. N. Bogdanov, and R. Wiesendanger, The properties of isolated chiral Skyrmions in thin magnetic films, New J. Phys. 18, 065003 (2016).

[7] R. Wiesendanger, Nanoscale magnetic Skyrmions in metallic films and multilayers: A new twist for spintronics, Nat. Rev. Mater. 1, 16044 (2016).

[8] A. Fert, N. Reyren, and V. Cros, Magnetic Skyrmions: advances in physics and potential applications, Nat. Rev. Mater. 2, 17031 (2017).

[9] A. Fert, V. Cros, and J. Sampaio, Skyrmions on the track, Nat. Nanotechnol. 8, 152 (2013).

[10] J. Sampaio, V. Cros, S. Rohart, A. Thiaville, and A. Fert, Nucleation, stability and current-induced motion of isolated magnetic Skyrmions in nanostructures, Nat. Nanotechnol. 8, 839 (2013).

[11] R. Tomasello, E. Martinez, R. Zivieri, L. Torres, M. Carpentieri, and G. Finocchio, A strategy for the design of Skyrmion racetrack memories, Sci. Rep. 4, 6784 (2014).

[12] X. Zhang, G. P. Zhao, H. Fangohr, J. P. Liu, W. X. Xia, J. Xia, and F. J. Morvan, Skyrmion-Skyrmion and Skyrmion-edge repulsions in Skyrmion-based racetrack memory, Sci. Rep. 5, 7643 (2015).

[13] S. Krause and R. Wiesendanger, Spintronics: Skyrmionics gets hot, Nat. Mater. 15, 493 (2016).

[14] W. Kang, Y. Huang, C. Zheng, W. Lv, N. Lei, Y. Zhang, X. Zhang, Y. Zhou, and W. Zhao, Voltage controlled magnetic Skyrmion motion for racetrack memory, Sci. Rep. 6, 23164 (2016).

[15] J. Müller, Magnetic Skyrmions on a two-lane racetrack, New J. Phys. 19, 025002 (2017).

[16] X. Zhang, M. Ezawa, and Y. Zhou, Magnetic Skyrmion logic gates: Conversion, duplication and merging of Skyrmions, Sci. Rep. 5, 9400 (2015).

[17] S. Mühlbauer, B. Binz, F. Jonietz, C. Pfleiderer, A. Rosch, A. Neubauer, R. Georgii, and P. Böni, Skyrmion lattice in a chiral magnet, Science 323, 915 (2009).

[18] X. Z. Yu, Y. Onose, N. Kanazawa, J. H. Park, J. H. Han, Y. Matsui, N. Nagaosa, and Y. Tokura, Real-space observation of a two-dimensional Skyrmion crystal, Nature (London) 465, 901 (2010).

[19] X. Z. Yu, N. Kanazawa, Y. Onose, K. Kimoto, W. Z. Zhang, S. Ishiwata, Y. Matsui, and Y. Tokura, Near room-temperature formation of a Skyrmion crystal in thin-films of the helimagnet fege, Nat. Mater. 10, 106 (2011).

[20] P. Milde, D. Köhler, J. Seidel, L. M. Eng, A. Bauer, A. Chacon, J. Kindervater, S. Mühlbauer, C. Pfleiderer, S. Buhrandt, C. Schütte, and A. Rosch, Unwinding of a Skyrmion lattice by magnetic monopoles, Science 340, 1076 (2013).

[21] U. K. Rößler, A. N. Bogdanov, and C. Pfleiderer, Spontaneous Skyrmion ground states in magnetic metals, Nature (London) 442, 797 (2006).

[22] M. Lee, W. Kang, Y. Onose, Y. Tokura, and N. P. Ong, Unusual Hall Effect Anomaly in MnSi Under Pressure, Phys. Rev. Lett. 102, 186601 (2009).

[23] A. Neubauer, C. Pfleiderer, B. Binz, A. Rosch, R. Ritz, P. G. Niklowitz, and P. Boni, Topological Hall Effect in the a Phase of MnSi, Phys. Rev. Lett. 102, 186602 (2009).

[24] N. Kanazawa, Y. Onose, T. Arima, D. Okuyama, K. Ohoyama, S. Wakimoto, K. Kakurai, S. Ishiwata, and Y. Tokura, Large Topological Hall Effect in a Short-Period Helimagnet MnGe, Phys. Rev. Lett. 106, 156603 (2011).

[25] Y. Li, N. Kanazawa, X. Z. Yu, A. Tsukazaki, M. Kawasaki, M. Ichikawa, X. F. Jin, F. Kagawa, and Y. Tokura, Robust Formation of Skyrmions and Topological Hall Effect Anomaly in Epitaxial Thin Films of MnSi, Phys. Rev. Lett. 110, 117202 (2013).

[26] D. A. Gilbert, B. B. Maranville, A. L. Balk, B. J. Kirby, P. Fischer, D. T. Pierce, J. Unguris, J. A. Borchers, and K. Liu, Realization of ground-state artificial Skyrmion lattices at room temperature, Nat. Commun. 6, 8462 (2015).

[27] L. Sun, R. X. Cao, B. F. Miao, Z. Feng, B. You, D. Wu, W. Zhang, A. Hu, and H. F. Ding, Creating an Artificial Two-Dimensional Skyrmion Crystal by Nanopatterning, Phys. Rev. Lett. 110, 167201 (2013).

[28] M. V. Sapozhnikov and O. L. Ermolaeva, Two-dimensional Skyrmion lattice in a nanopatterned magnetic film, Phys. Rev. B 91, 024418 (2015).

[29] M. V. Sapozhnikov, S. N. Vdovichev, O. L. Ermolaeva, N. S. Gusev, A. A. Fraerman, S. A. Gusev, and Yu. V. Petrov, Artificial dense lattice of magnetic bubbles, Appl. Phys. Lett. 109, 042406 (2016).

[30] M. V. Sapozhnikov, Skyrmion lattice in a magnetic film with spatially modulated material parameters, J. Magn. Magn. Mater. **396**, 338 (2015).

[31] M. Beg, R. Carey, W. Wang, D. Cortés-Ortuño, M. Vousden, M.-A. Bisotti, M. Albert, D. Chernyshenko, O. Hovorka, R. L. Stamps, and H. Fangohr, Ground state search, hysteretic behaviour, and reversal mechanism of Skyrmionic textures in confined helimagnetic nanostructures, Sci. Rep. **5**, 17137 (2015).

[32] J. Mulkers, B. Van Waeyenberge, and M. V. Milošević, Effects of spatially engineered Dzyaloshinskii-Moriya interaction in ferromagnetic films, Phys. Rev. B **95**, 144401 (2017).

[33] W. Jiang, P. Upadhyaya, W. Zhang, G. Yu, M. B. Jungfleisch, F. Y. Fradin, J. E. Pearson, Y. Tserkovnyak, K. L. Wang, O. Heinonen, S. G. E. te Velthuis, and A. Hoffmann, Blowing magnetic Skyrmion bubbles, Science **349**, 283 (2015).

[34] G. Chen, A. Mascaraque, A. T. N'Diaye, and A. K. Schmid, Room temperature Skyrmion ground state stabilized through interlayer exchange coupling, Appl. Phys. Lett. **106**, 242404 (2015).

[35] A. Kákay, E. Westphal, and R. Hertel, Speedup of FEM micromagnetic simulations with graphical processing units, IEEE Trans. Magn. **46**, 2303 (2010).

[36] Y. S. Lin, P. J. Grundy, and E. A. Giess, Bubble domains in magnetostatically coupled garnet films, Appl. Phys. Lett. **23**, 485 (1973).

[37] T. Garel and S. Doniach, Phase transitions with spontaneous modulation-the dipolarizing ferromagnet, Phys. Rev. B **26**, 325 (1982).

[38] A. P. Malozemoff and J. C. Slonzewski, *Magnetic Domain Walls in Bubble Materials* (Academic Press, New York, 1979).

[39] N. S. Kiselev, A. N. Bogdanov, R. Schäfer, and U. K. Rößler, Chiral Skyrmions in thin magnetic films: new objects for magnetic storage technologies?, J. Phys. D **44**, 392001 (2011).

[40] Ar. Abanov and V. L. Pokrovsky, Skyrmion in a real magnetic film, Phys. Rev. B **58**, R8889 (1998).

[41] A. O. Leonov and M. Mostovoy, Multiply periodic states and isolated Skyrmions in an anisotropic frustrated magnet, Nat. Commun. **6**, 8275 (2015).

[42] S.-Z. Lin and S. Hayami, Ginzburg-landau theory for Skyrmions in inversion-symmetric magnets with competing interactions, Phys. Rev. B **93**, 064430 (2016).

[43] E. A. Stepanov, C. Dutreix, and M. I. Katsnelson, Dynamical and Reversible Control of Topological Spin Textures, Phys. Rev. Lett. **118**, 157201 (2017).

[44] A. N. Bogdanov and D. A. Yablonskiǐ, Thermodynamically stable "vortices", in magnetically ordered crystals. The mixed state of magnets, JETP, **68**, 101 (1989).

[45] A. Bogdanov and A. Hubert, Thermodynamically stable magnetic vortex states in magnetic crystals, J. Magn. Magn. Mater. **138**, 255 (1994).

[46] A. Bogdanov and A. Hubert, The stability of vortex-like structures in uniaxial ferromagnets, J. Magn. Magn. Mater. **195**, 182 (1999).

[47] A. N. Bogdanov and U. K. Rößler, Chiral Symmetry Breaking in Magnetic Thin Films and Multilayers, Phys. Rev. Lett. **87**, 037203 (2001).

[48] S. Komineas and N. Papanicolaou, Skyrmion dynamics in chiral ferromagnets, Phys. Rev. B **92**, 064412 (2015).

[49] A. Crépieux and C. Lacroix, Dzyaloshinsky–Moriya interactions induced by symmetry breaking at a surface, J. Magn. Magn. Mater. **182**, 341 (1998).

[50] A. Thiaville, S. Rohart, É. Jué, V. Cros, and A. Fert, Dynamics of Dzyaloshinskii domain walls in ultrathin magnetic films, Europhys. Lett. **100**, 57002 (2012).

[51] H. Yang, A. Thiaville, S. Rohart, A. Fert, and M. Chshiev, Anatomy of Dzyaloshinskii-Moriya Interaction at Co/Pt Interfaces, Phys. Rev. Lett. **115**, 267210 (2015).

[52] S. Rohart and A. Thiaville, Skyrmion confinement in ultrathin film nanostructures in the presence of Dzyaloshinskii-Moriya interaction, Phys. Rev. B **88**, 184422 (2013).

[53] Y. Gaididei, V. P. Kravchuk, and D. D. Sheka, Curvature Effects in Thin Magnetic Shells, Phys. Rev. Lett. **112**, 257203 (2014).

[54] D. D. Sheka, V. P. Kravchuk, and Y. Gaididei, Curvature effects in statics and dynamics of low dimensional magnets, J. Phys. A **48**, 125202 (2015).

[55] V. P. Kravchuk, U. K. Rößler, O. M. Volkov, D. D. Sheka, J. van den Brink, D. Makarov, H. Fuchs, H. Fangohr, and Y. Gaididei, Topologically stable magnetization states on a spherical shell: Curvature-stabilized Skyrmions, Phys. Rev. B **94**, 144402 (2016).

[56] Another type of DMI may lead to a spiral-like Skyrmion, which is intermediate between Néel and Bloch types. This case requires an extra analysis.

[57] In other words, the magnetostatic contribution is replaced by an effective easy-surface anisotropy [58–61], which simply results in a shift of the anisotropy constant K.

[58] V. Slastikov, Micromagnetism of thin shells, Math. Models Methods Appl. Sci. **15**, 1469 (2005).

[59] G. Gioia and R. D. James, Micromagnetics of very thin films, Proc. R. Soc. A **453**, 213 (1997).

[60] R. V. Kohn and V. V. Slastikov, Effective dynamics for ferromagnetic thin films: A rigorous justification, Proc. R. Soc. A **461**, 143 (2005).

[61] R. V. Kohn and V. V. Slastikov, Another thin-film limit of micromagnetics, Arch. Ration. Mech. Anal. **178**, 227 (2005).

[62] See Supplemental Material at http://link.aps.org/supplemental/10.1103/PhysRevLett.120.067201 for details of mathematical calculations and micromagnetic simulations, which includes Refs. [63–65].

[63] R. Kamien, The geometry of soft materials: A primer, Rev. Mod. Phys. **74**, 953 (2002).

[64] M. J. Bowick and L. Giomi, Two-dimensional matter: Order, curvature and defects, Adv. Phys. **58**, 449 (2009).

[65] A. Bogdanov and A. Hubert, The properties of isolated magnetic vortices, Physica (Amsterdam) **186B**, 527 (1994).

[66] A. A. Belavin and A. M. Polyakov, Metastable states of a 2D isotropic ferromagnet, JETP Lett. **22**, 245 (1975).

[67] Note that the sign of each of the quantities $\mathcal{H}$ and D separately is not physically fixed, because it is determined by the chosen direction of the normal vector $\boldsymbol{n}$.

[68] If solution $\boldsymbol{m}$ is stable then solution $-\boldsymbol{m}$ is also stable, see Sec. S.IV.

[69] The same invariance takes place for the transformation $k_i \to -k_i$, $d \to -d$, $\Theta \to 2\pi - \Theta$. This property is reflected in the symmetry of the diagram of Skyrmion states, see Fig. 3.

[70] K. V. Yershov, V. P. Kravchuk, D. D. Sheka, and Y. Gaididei, Curvature-induced domain wall pinning, Phys. Rev. B **92,** 104412 (2015).

[71] Skyrmion radius R is determined as solution of equation $\cos \Theta(R) = 0$. For the parameters of Fig. 1 the small and big Skyrmion radii are $R_{sml} \approx 0.14$ and $R_{big} \approx 3.7$, respectively; $\mathcal{K}(s)$ has extreme points $s_1 = 0$ and $s_2 \approx 3.3$.

[72] V. Vitelli and A. M. Turner, Anomalous Coupling Between Topological Defects and Curvature, Phys. Rev. Lett. **93,** 215301 (2004).

[73] A. M. Turner, V. Vitelli, and D. R. Nelson, Vortices on curved surfaces, Rev. Mod. Phys. **82,** 1301 (2010).

[74] V. L. Carvalho-Santos, R. G. Elias, D. Altbir, and J. M. Fonseca, Stability of Skyrmions on curved surfaces in the presence of a magnetic field, J. Magn. Magn. Mater. **391,** 179 (2015).

[75] V. L. Carvalho-Santos, F. A. Apolonio, and N. M. Oliveira-Neto, On geometry–dependent vortex stability and topological spin excitations on curved surfaces with cylindrical symmetry, Phys. Lett. A **377,** 1308 (2013).

[76] P. S. C. Vilas-Boas, R. G. Elias, D. Altbir, J. M. Fonseca, and V. L. Carvalho-Santos, Topological magnetic solitons on a paraboloidal shell, Phys. Lett. A **379,** 47 (2015).

[77] D. Makarov, L. Baraban, I. L. Guhr, J. Boneberg, H. Schift, J. Gobrecht, G. Schatz, P. Leiderer, and M. Albrecht, Arrays of magnetic nanoindentations with perpendicular anisotropy, Appl. Phys. Lett. **90,** 093117 (2007).

[78] D. Makarov, P. Krone, D. Lantiat, C. Schulze, A. Liebig, C. Brombacher, M. Hietschold, S. Hermann, C. Laberty, D. Grosso, and M. Albrecht, Magnetization reversal in arrays of magnetic nanoperforations, IEEE Trans. Magn. **45,** 3515 (2009).

[79] C. Brombacher, M. Saitner, C. Pfahler, A. Plettl, P. Ziemann, D. Makarov, D. Assmann, M. H. Siekman, L. Abelmann, and M. Albrecht, Tailoring particle arrays by isotropic plasma etching: an approach towards percolated perpendicular media, Nanotechnology **20,** 105304 (2009).

[80] R. Streubel, P. Fischer, F. Kronast, V. P. Kravchuk, D. D. Sheka, Y. Gaididei, O. G. Schmidt, and D. Makarov, Magnetism in curved geometries (topical review), J. Phys. D **49,** 363001 (2016).

[81] M. Finazzi, M. Savoini, A. R. Khorsand, A. Tsukamoto, A. Itoh, L. Duò, A. Kirilyuk, Th. Rasing, and M. Ezawa, Laser-Induced Magnetic Nanostructures with Tunable Topological Properties, Phys. Rev. Lett. **110,** 177205 (2013).

[82] Y. Liu, H. Du, M. Jia, and A. Du, Switching of a target Skyrmion by a spin-polarized current, Phys. Rev. B **91,** 094425 (2015).

[83] A. O. Leonov, U. K. Rößler, and M. Mostovoy, Target-Skyrmions and Skyrmion clusters in nanowires of chiral magnets, Eur. Phys. J. Web Conf. **75,** 05002 (2014).

[84] R. Dandoloff, S. Villain-Guillot, A. Saxena, and A. R. Bishop, Violation of Self-Duality for Topological Solitons Due to Soliton-Soliton Interaction on a Cylindrical Geometry, Phys. Rev. Lett. **74,** 813 (1995).

[85] S. Villain-Guillot, R. Dandoloff, A. Saxena, and A. R. Bishop, Topological solitons and geometrical frustration, Phys. Rev. B **52,** 6712 (1995).

[86] A. Saxena and R. Dandoloff, Curvature-induced geometrical frustration in magnetic systems, Phys. Rev. B **55,** 11049 (1997).

[87] A. Saxena, R. Dandoloff, and T. Lookman, Deformable curved magnetic surfaces, Physica (Amsterdam) **261A,** 13 (1998).

[88] A. Saxena and R. Dandoloff, Heisenberg spins on a cylinder in an axial magnetic field, Phys. Rev. B **58,** R563 (1998).